Excerpt from the Proceedings of the 2011 COMSOL Conference in Boston

Analyzing Drug Delivery and Osteoblast Growth on a Porous Scaffold in a Perfusion Bioreactor

Argus Sun*[1,2], Samuel S. Murray[1,2,3]
[1]Department of Biomedical Engineering, UCLA, [2]VA Greater Los Angeles Healthcare System, [3]Department of Medicine, UCLA
*Corresponding Author: argus@seas.ucla.edu or argus.sun@gmail.com

Abstract: Implantable Collagen sponges are used in Spinal Surgery as Drug Delivery Scaffolds. An optimal concentration of growth factor that strikes a balance between bone growth and adverse diffusion effects is difficult to find. The porous sponge also serves as a scaffold for Osteoblast growth, and fluid shear has been shown to mediate biological effects on that cell type. We use Comsol Multiphysics to model an in vitro perfusion bioreactor system that contains a porous scaffold in the reaction chamber. The reaction engineering interface is used to model release of scaffold-bound growth factor, while its subsequent convection and diffusion are modeled as species transport in porous media. The Brinkman Equations are used to simulate fluid flow through the Porous phase.

Keywords: Drug delivery, Porous flow, Bioreactor, Convection and Diffusion

1. Introduction

Porous collagen sponges loaded with growth factors are used in spinal surgery to promote bone growth at the site where they are applied. In spinal fusion procedures the absorbable collagen sponges are soaked with a solution containing growth factors, such as recombinant human bone morphogenetic protein 2 (rhBMP-2), prior to implantation. While soaked sponges are effective in mediating bone mineralization around the vertebrae being joined, the unwanted side effect of ectopic bone growth[1] sometimes occurs at distant sites. This is thought to be due to diffusion of BMP-2 away from the sponge post-implantation[2]. One solution would be to adjust dosage of BMP-2, but an optimal concentration where desired and unwanted effects are balanced could be difficult to find. Person to person anatomical variation is one factor complicating dose optimization. A different solution would be to control the release of the loaded growth factor. In this paper we model, using the finite element method, release of BMP-2 from a collagen sponge in a perfusion bioreactor[4]. To model cellular infiltration, we track growth on the sponge through changes of its physical characteristics stemming from function as a scaffold for cell growth. We use MC3T3 E1 mouse calvarial cells, a well-characterized osteogenic cell line[7]. The strategy used to slow release is to functionalize the fluid-exposed surface of the sponge with proteins and peptides that bind with different affinities[3] to the growth factor of interest, BMP-2.

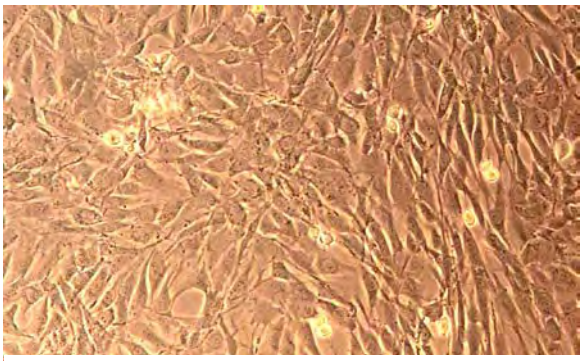

Figure 1 Day 3 MC3T3E1 Mouse Calvarial Cells

2. Use of Comsol Multiphysics

2.1 Model & Governing Equations

Fluid flow through the reactor is governed by Equation 1, a version of the Navier-Stokes equations with terms included to describe porous media:

$$\nabla \cdot \left[\frac{\eta}{\varepsilon}(\nabla \mathbf{u} + (\nabla \mathbf{u})^{T}) + p\mathbf{I}\right] = \frac{\eta}{\kappa}\mathbf{u} \quad (1a)$$

$$\nabla \cdot \mathbf{u} = 0 \qquad (1b)$$

With boundary conditions:

$\mathbf{u}\cdot\mathbf{n} = u_o$, inlet; $\mathbf{u} = \mathbf{0}$, walls; p = 0 , outlet

The scalar coefficients p, η, κ, ε are the pressure, viscosity, permeability and the porosity, with respect to order. The porosity is a dimensionless ratio between the void volume and the total volume. To avoid reactor washout[8] prior to cell attachment, initial velocities were chosen on the basis of the residence time τ_{res} generated, as follows:

$$\tau_{res} = \frac{a u_o}{V} \qquad (2)$$

Where variable a is the inlet cross-sectional area, u_o the initial velocity at the inlet and V the total volume of the reactor. This prediction follows from restriction on fluid compression in equation 1b.

The effect of cell growth is described by pore shrinkage from crowding (fig 1A). The following equation characterizes the resulting decrease in porosity:

$$\varepsilon(t) = \varepsilon_o\left(1 - \frac{m e^{\mu t}}{\rho_c V_s}\right) \qquad (3)$$

The terms ε_o, m, μ, ρ_c, V_s are acellular porosity, mass per cell, log phase growth rate, density of cellular material, and the volume of the scaffold, respectively. A constant μ was used because fluctuations should be negligible during time scales on the same order of magnitude as the doubling time. The accumulation of cellular matter on the sponge decreases ε through the negative term in the preceding equation. This decrease in porosity can be treated as porous phase deposition[11] described by the following power law:

$$\kappa \approx \kappa_o\left(\frac{\varepsilon(t)}{\varepsilon_o}\right)^{3.55} \qquad (4)$$

The release of growth factor bound to the sponge is dependent on the affinity of the binding molecule-growth factor interaction. Binding kinetics governing the behavior of bound and free protein growth factor are modeled as two separate chemical species to facilitate independent treatment for mass transport. The rate equations are shown here:

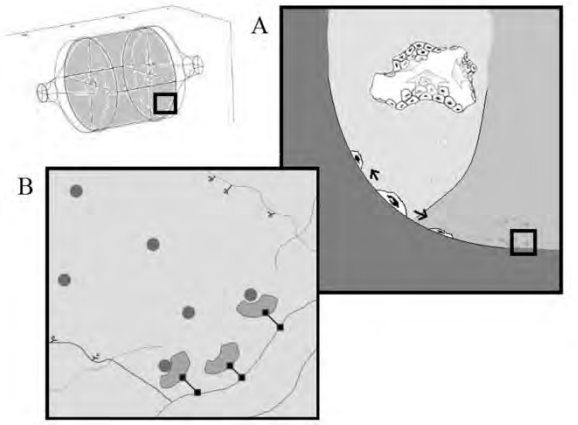

Figure 2 A. Cell Growth and B. Growth Factor Release

$$\frac{dC_{BMP-2,free}}{dt} = R_1 = k_d C_{BMP-2,bound} - k_a C_{BMP-2,free}(C_o - C_{BMP-2,bound}) \qquad 5(a)$$

$$\frac{dC_{BMP-2,bound}}{dt} = R_2 = k_a C_{BMP-2,free}(C_o - C_{BMP-2,bound}) - k_d C_{BMP-2,bound} \qquad 5(b)$$

Finally, mass transport in the system is described by the convection-diffusion equations:

$$\frac{\partial c_i}{\partial t} + \nabla \cdot \left(-D_{i,sbd}\nabla c_i + \xi c_i \mathbf{u}\right) = R_i \qquad (6)$$

The diffusivity D has values particular to the species in question and the media phase they diffuse through. The convection term has velocity **u** from equation 1 and coefficient ξ , a unit step function for binding to the porous phase. The reaction term R is from Equation 5.

2.2 Geometry

The geometry (figure 2, top left) was designed to house the collagen sponge with dimensions identical to bioassay[2] implants. The inlet and outlet were designed to fit peristaltic pump tubing. To prevent eddy formation from sharp corners, a spline was drawn from inlet to the bulk of the reactor. The cross section was then revolved to form the final geometry. To facilitate insertion or removal of the sponge, a sealable notch can be created along the perimeter of the reactor chamber, this liquid-tight seal would not affect the interior geometry. Low flow rates necessary to generate long residence times also require gas permeable materials in fabrication.

2.3 Parameters

The parameters used in simulation were derived from literature or obtained experimentally. Covalently cross-linked Collagen I Sponges were purchased from Integra (Plainsboro, New Jersey) and characterized by fluid displacement for porosity measurement. The sponges were subject to H&E staining, paraffin embedding and histological sectioning for pore size determination. The Bruggeman permeability from was obtained by multiplying the hydraulic conductivity[5] with the viscosity[6] of glutaraldehyde cross-linked Collagen I. MC3T3E1 clone 4 cells were obtained from ATCC (Manassas, Virginia) and grown starting from passage 8, Cell mass measurements were taken at 24, 48 and 72 hours and confirmed by amount of total protein[8] through BCA Protein assay. Cell volume was also determined through examination of day 4 confluent culture micrographs[7].

Table 1 Parameter List

Parameter	Description	Value
η	Viscosity perfusion media	$1x10^{-3}$ Pa·s
a	Inlet Area	1.957 mm^2
u_o	Inlet Velocity	4.364 μm/s
ε_o	Porosity -sponge only	0.9
m	Mass per cell	10.397 ng
μ	Cell Growth Rate	1.070 s^{-1}
ρ_c	Cell Mass Density	1.023 g/cm^3
V_s	Scaffold Volume –quarter	0.07453 cm^3
κ_o	Permeability -sponge only	9.7249 m^2
$D_{1,1}$	Diffusivity of free BMP-2	$13x\ 10^{-7} cm^2/s$
$D_{1,2}$	Diffusivity of free BMP-2 (Porous Phase)	$11x10^{-7}\ cm^2/s$
$D_{2,2}$	Diffusivity of bound BMP-2	$0.66x10^{-7} cm^2/s$
C_o	Initial Bound BMP-2	7.982 μM

Inlet velocity required some optimizing—the resulting velocity was chosen to match residence time in the reactor to cell doubling time (18hrs).

The diffusion constant for cytochrome C[9] was used because its molecular weight is nearly identical to monomeric rhBMP-2 (12.31 kDa vs. 12.53 kDa). The tortuosity and microstructure of the sponge will likely influence diffusion, so diffusity was multiplied by a coefficient slightly lower than the porosity for $D_{1,2}$. Rather than treat the scaffold bound BMP-2 as linked to a large inert crosslinked macromolecule, we assumed that the crosslinks allow relatively free range of motion by acting as a tether. To reflect local concentration fluctuations we treated the collagen bound complex of BMP-2 and binding protein as a single entity, and because the aspect ratio of collagen-I dominates, the porosity limited diffusivity of a collagen-I monomer[10] was used. Initial concentration of BMP-2 was based on the effective dose[2] from bioassay.

Three molecules spanning a range of binding affinities[2,3] to BMP-2 were used to test release rates of the growth factor from the scaffold.

Table 2 Binding Affinities

Protein	Affinity	Value
bspp24 (full length)	k_d	$2.29x10^{-3}\ s^{-1}$
	k_a	$3.86x10^5$ L/mol·s
spp14.5 (truncated)	k_d	$3.60x10^{-3}\ s^{-1}$
	k_a	$1.53x10^4$ L/mol·s
cBBP (peptide)	k_d	$0.72x10^{-3}\ s^{-1}$
	k_a	$1.35x10^5$ L/mol·s

2.4 Simulation

The convection-diffusion (chcd), diffusion (chdi) and Brinkman (chns) equation modules were used. The flow module was stationary while the other two were transient. Prior to running time-dependent simulation, a parameter sweep at a single time point was performed to find the optimal inlet velocity. Time-dependent runs stretching 18 hours with time steps of 30 minutes were then performed with each binding protein. Simulations would converge consistently when extended up to 14 days. For speed, the geometry was quartered and two symmetry boundary conditions applied. Coarser meshes of 10,790 elements proved sufficient. The iterative solver used was Biconjugate Gradient Stability method. Incomplete LU was used as a preconditioner with a tolerance of 0.15 and a drop tolerance of $1x10^{-5}$ in relation to fill-in. Simulation was performed on a Dual 2.394 GHz Intel Xeon workstation with 32 GB RAM and on a Intel Pentium i7 Ideapad with 8 GB of RAM. Versions 3.5a and 4.2 of Comsol multiphysics were used. Computational time averaged 71 minutes.

Figure 3 Porosity Plot

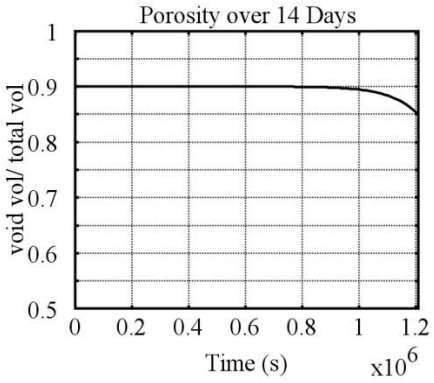

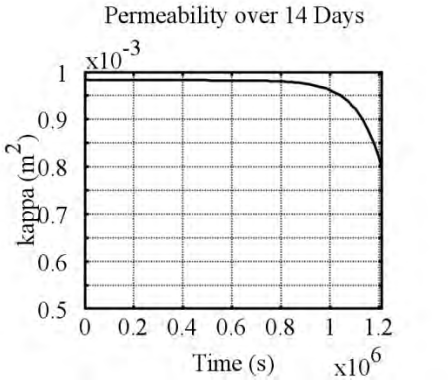

Figure 4 Permeability Plot

Figure 5 bFLspp24 Conc Distribution

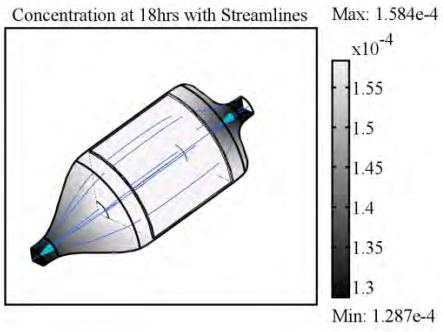

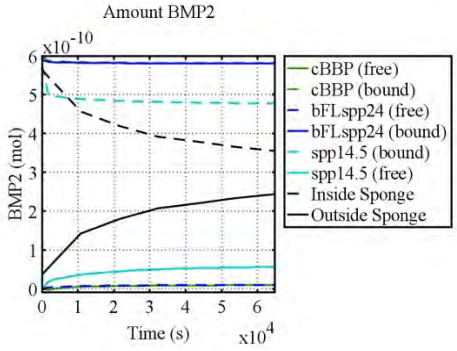

Figure 6 BMP-2 Delivery

3. Results and Discussion

Cell growth did not affect porosity significantly within the doubling time of 18 hrs, however when continued to 14 days, ε(t) drops to a value of 0.85 (figure 3). The higher order power law dependence of κ shows a faster rate of decline noticeable within the doubling time (figure 4). However the change in permeability was not dramatic enough to create a significant alteration in flow pattern at either 18 hours or 14 days, though the streamline profile did shift nominally. One reason for this is likely because the sloping increase of cross-sectional area within the geometry slows flow to an almost stagnant velocity, stifling all but the largest velocity shifts. An analogy seen in physiology would be slowing in blood flow during transition from arteriole to capillary. In earlier simulations done with lower porosity scaffolds such as chitosan[4], flow is channeled around the porous phase and speeds up significantly in the small gap between the porous phase and the wall.

In evaluating different binding proteins' effect on BMP-2 release, the trend of fastest release was headed by spp14.5 followed by FLbspp24 with cBBP peptide closely behind (Figure 6). It should be noted that all binding molecules are significantly below sponge alone. At the end of 18 hr simulation, concentration of BMP-2 in the sponge system have nearly equilibrated throughout the entire reactor volume, while systems with binding peptide or proteins have retained a reservoir of BMP-2 within the sponge compartment. In the distribution slice and boundary plot (Figure 5), ends of the sponge exposed to larger volumes of the longitudinal ends of the flow chamber have released much more BMP-2 compared to a radial distribution. In the supplementary animations where the plots are rotated, it is possible to see the extent of how porous phase flow impedance distorts streamlines.

4. Conclusion

The simulations have demonstrated potential for this bioreactor design to be used to evaluate the kinetics of osteobiologic delivery with collagen sponges modified by binding proteins. The model is limited in length of simulation by the accurate depiction of biological response. As currently modeled, cell growth rate is constant, while MC3T3s in tissue culture display marked changes in growth rate during differentiation to osteoblast phenotype. The rate of that differentiation is in turn responsive to BMP-2 concentration. Extraction of cells to determine their differentiation state at different time points will elucidate further parameters regarding growth rate.

5. Acknowledgements

Special thanks to Elsa B. Murray, Ke-Wei Zhao and Louis Bouchard for their technical and scientific advice as well as Mina Sierou from Comsol for her assistance.

6. References

1. Mroz, T.; Wang, J.; Hashimoto, R. Complications Related to Osteobiologics Use in Spine Surgery, *SPINE*, **Volume 35**, pp S86-S104 (2010)

2. Sintuu, C.; Murray, S.; Behnam, K.; Simon, R.; Jawien, J.; Silva, J.; Duarte M.; Brochmann, E. Full-Length Bovine spp24 [spp24 (24-203)] Inhibits BMP-2 Induced Bone Formation, *J Orthop Research* , **Volume 26(6)**, pp. 753-58 (2008)

3. Sun, A.; Murray, S.; Simon, R.; Jawien J.; Behnam K.; Miller, T.; Brochmann, E. Alanine-Scanning Mutations of the BMP-binding Domain of Recombinant Secretory bovine spp24 Affect Cytokine Binding, *Connect Tissue Res*, **Volume 51**, pp. 445-51 (2010)

4. Lawrence, B.; Devarapalli, M.; Madihally, S. Flow Dynamics in Bioreactors Containing Tissue Engineering Scaffolds, *Biotechnology and Bioengineering*, **Volume 102**, pp. 935-47 (2008)

5. Borene, M.; Barocas, V.; Hubel, A. Mechanical and Cellular Changes during Compaction of a Collagen-Sponge-Based Corneal Stromal Equivalent, *Annals of Biomedical Engineering*, **Volume 32**, pp. 274–283 (2004)

6. Chan, R.; Titze, I. Viscosities of Implantable Biomaterials in Vocal Fold Augmentation Surgery, *The Laryngoscope*, **Volume 108**, pp. 725-31 (1998)

7. Sudo, H.; Kodama, H.; Amagai, Y.; Yamamoto, S. In Vitro Differentiation and Calcification in a New Clonal Osteogenic Cell Line Derived fron Newborn Mouse Calvaria, *J Cell Biol*, **Volume 96**, pp. 191-98 (1983)

8. Blanch, H.; Clark, D.; *Biochemical Engineering*, Marcel Dekker, New York, pp. 209-19(1997)

9. Truskey, G.; Yuan, F.; Katz, D. *Transport Phenomena in Biological Systems*, Pearson Prentice-Hall, New Jersey, pp. 276-81 (2004)

10. Gelman, R.; Piez, K. Collagen Fibril Formation In Vitro. A Quasielastic Light-Scattering Study of Early Stages, *J Biol Chem*, **Volume 255(17)**, 8098-102, (1980)

11. Borisova, E.; Adler, P. Deposition in Porous Media and Clogging on the Field Scale, *Physical Review E*, **Volume 71,** pp. 0163111-19 (2005),

7. Appendix

Animations created of simulations from this article can be found at the following URL:

http://asun.bol.ucla.edu/simulation/animations.html